

Received 00th January 20xx,

Luminescence in the Solid State of Phosphine-EWO Ligands with Fluorinated Chalcone Skeletons and their PdX₂ complexes. Metal-promoted Phosphorescence Enhancement

Jaime Ponce-de-León,^a Marconi N. Peñas-Defrutos,^{a,*} Andrea Vélez,^a Gabriel Aullón,^b and Pablo Espinet^{a,*}

Accepted 00th January 20xx

DOI: 10.1039/x0xx00000x

www.rsc.org/

***trans*-[PdX₂L₂] complexes (X = Cl, Br; L = R-PEWO-F₄) display remarkable phosphorescent emission in the solid state, which is not observed when using CN⁻ instead of halide, or Pt instead of Pd. DFT calculations explain these observations, illustrating the drastic effect of the metal moieties on the frontier orbitals of these structurally identical derivatives: hybridization of the moderately stable orbitals of the PdX₂ core with those of the chalcone fragment of the ligands is found only for the LUMO of the emissive compounds. Attending to their substantially lower lifetimes, the free ligands feature fluorescent behaviour.**

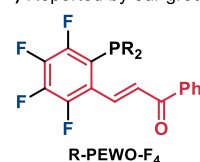
Chalcone derivatives (Ar-CH=CH-CO-Ar') are mainly known due to their biologic activity and pharmacological applications,¹ but some of them display interesting photophysical properties as well.² These compounds typically exhibit aggregation induced emission, determined by their lack of planarity that hinders π -stacking interactions and by *push-pull* conjugation effects at the enone moiety.³ Very recently, a rare crystal jumping behavior was found for a highly luminescent chalcone derivative, due to a reversible intermolecular [2+2] cycloaddition process in the solid state.⁴ Chemosensors with chalcone-based chromophores have been applied for the selective detection of Cu²⁺ in aqueous media.⁵ Applications of chalcone-derived liquid crystals for NH₃(g) sensing are also worth mentioning.⁶

Our pursuit of designing hemilabile ligands able to promote challenging Pd-catalysed C-C couplings (e.g. Ar^F-Ar^F, Ar^F = fluorinated aryl), led us to develop a family of fluorinated PEWO ligands showed in Figure 1A (PEWO = Phosphine bearing Electron-Withdrawing Olefins). The previously

synthesized L^{1,9}, L^{2,10} and L³ (reported here for the first time) differ in the PR₂ moiety (R = Ph, Cy, iPr respectively), while the analogue of L¹ without fluorine substitution, labelled as L⁴, was reported by Lei *et al.* (Figure 1B).¹¹ Clearly, these PEWO ligands feature a chalcone skeleton (highlighted in red in Figure 1).

Remarkably, the hybrid chelating ligand L¹ is extremely efficient in lowering the reductive elimination barrier and also allow for oxidative addition with either ArI or ArBr (ArCl cannot be used) in catalytic conditions.^{15,16} Particularly, complex [PdCl₂L¹] (2L¹) is an active catalyst for Negishi heterocoupling of fluorinated aryls.¹⁷ A detailed mechanistic study of the synthesis of the [PdCl₂Lⁿ] (2Lⁿ) complexes showed that the reaction of one equivalent of L (*E*-configuration) with *trans*-[PdCl₂(NCMe)₂] quickly produces *trans*-[PdCl₂(Lⁿ)₂] (1Lⁿ, Lⁿ = L¹, L²), observed as an intermediate in the reaction (Scheme 1).⁸ The coexistence of the starting materials and complexes 1Lⁿ leads to ligand rearrangement and formation of the *E*-chelated complex (*E*-2Lⁿ), which subsequently isomerizes to the *Z* isomer, obtained selectively for L¹ (2L¹). The *Z*-configuration of the ligand eventually triggers a C-F activation process that opens the gate to new reactivity.²¹

A) Reported by our group

R = Ph (L¹); Cy (L²); iPr (L³)*

B) Reported by Lei

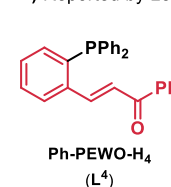


Fig. 1. Hybrid Phosphine-EWO ligands used in this work with the chalcone group highlighted in red. *L³ has not been previously reported.

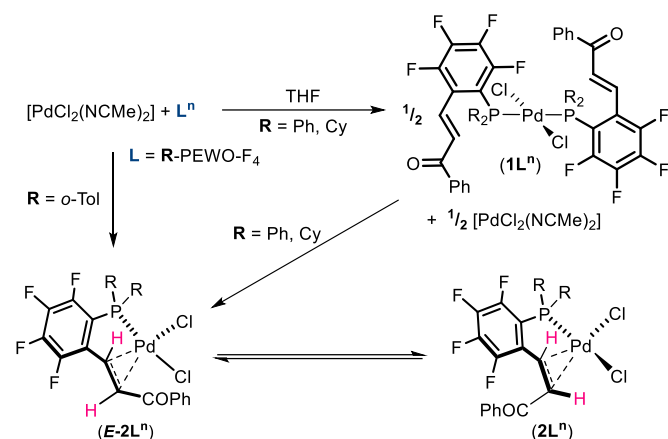
The remarkably low activation barrier for *E/Z* olefin-isomerization (it occurs at RT) supports an extraordinary electronic delocalization of the double bond into both extremes (C₆F₄ and COPh) of these fluorinated chalcone structures.^{8,22} The latter confirms the special *pull-pull* conjugation in our PEWO-F₄ ligands, that is tightly related with

^a IU CINQUIMA/Química Inorgánica, Facultad de Ciencias, Universidad de Valladolid, 47071-Valladolid, Spain. E-mail: marconi_44@hotmail.com espinet@qi.uva.es

^b Departament de Química Inorgànica, Universitat de Barcelona, Martí i Franquès 1-11, E-08028 Barcelona, (Spain).

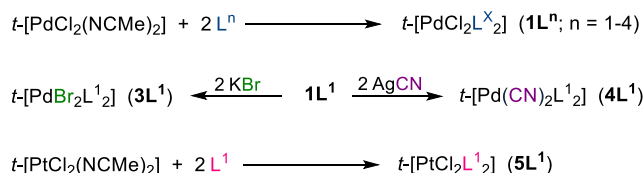
Electronic Supplementary Information (ESI) available: [synthesis and characterization of the complexes including NMR spectra, computational details and X-ray data]. CCDC 2205013-2205017. See DOI: 10.1039/x0xx00000x

the solid-state luminescence reported in this work, displayed by the free ligands and some of their metal complexes.



Scheme 1. Observed intermediates in the synthesis of $[\text{PdCl}_2\text{L}^n]$ (2L^n) complexes.

Complexes 1L^{1-4} were selectively prepared by reaction of *trans*- $[\text{PdCl}_2(\text{NCMe})_2]$ with two equivalents of the appropriate ligand (Scheme 3, see ESI for details). X-ray structures of 1L^1 ,⁷ 2L^1 ,⁷ L^2 ,⁸ and 1L^4 ,²⁴ were already available in the literature and those of 1L^2 and 1L^3 (Figures 2 and ESI1, respectively) are reported here. The crystalline structure of ligand Ph-PEWO- F_4 (L^1) is also first reported in this work (Figure ESI1). Treatment of 1L^1 with KBr or AgCN leads to *trans*- $[\text{PdBr}_2(\text{L}^1)_2]$ (3L^1) and *trans*- $[\text{Pd}(\text{CN})_2(\text{L}^1)_2]$ (4L^1), respectively. The platinum compound *trans*- $[\text{PtCl}_2(\text{L}^1)_2]$ (5L^1) is synthesized analogously to 1L^1 (Scheme 2).



Scheme 2. Synthesis of complexes 1L^n , 3L^1 , 4L^1 and 5L^1 . Note that all are *trans* compounds.

The fluorinated ligands L^1 and L^2 show yellow emission in the solid state upon UV irradiation, and the *E*-complexes 1L^{1-3} (and 3L^1) show eye-catching orange luminescence in similar conditions (Figure 2). However, the chelated *Z*-complex 2L^1 does not feature emissive properties. Neither the free ligands nor their complexes display emitting behaviour in solution.²⁵ Lack of fluorination is clearly detrimental for the luminescence (see quantum yield percentages for L^4 and 1L^4 in Table 1) and more interestingly, both 4L^1 and 5L^1 complexes, which do not show any remarkable structural differences with 1L^1 are not luminescent. Figure ESI2 compare those three X-ray structures, including relevant distances within the chalcone ring (*i.e.* -C=C-) and involving the metal centres.

Table 1 collects the experimental data (excitation and emission maxima, average lifetimes, and quantum yield percentages) measured for the luminescent crystalline solids. The emission spectra as well as the decay profiles are given in the ESI

(Figures ESI4-ESI13).²⁶ Excluding chelated *Z* complex 2L^1 , non-luminescent and with a drastic structural divergence, in all the other compounds (free ligands and complexes) the uncoordinated olefins have *E*-configuration. The chalcone moieties are submitted in the free ligands to orbital influences by the R substituents at the P atom, and, additionally, by the MX_2 metal fragment at which the phosphine is coordinated to in the complexes.

Concerning the free ligands, with different electronic and steric features, the highest maxima wavelength ($\lambda_{\text{emis}} = 606$ nm) is found for the fluorinated L^1 (R = Ph). For the fluorinated L^2 (R = Cy, $\lambda_{\text{emis}} = 552$ nm) the wavelength is closer to the value in L^4 (R = Ph) than in L^1 , as if the higher inductive effect of Cy acting as σ -donor towards the P atom was compensating, at the chalcone aryl, the electron withdrawing effect of fluorination. Apparently the two effects that increase the σ -electron density at the chalcone ring (non-fluorination and inductive effect from R) happen to diminish noticeably the quantum yield Φ values, to almost extinction in L^4 .

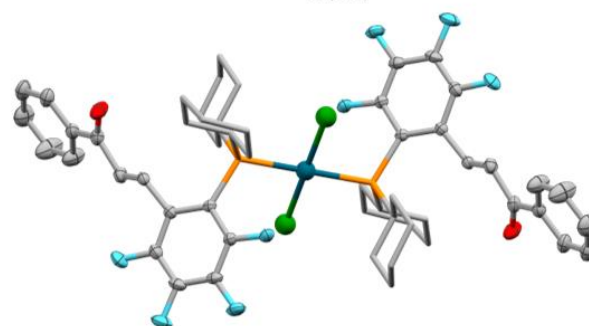
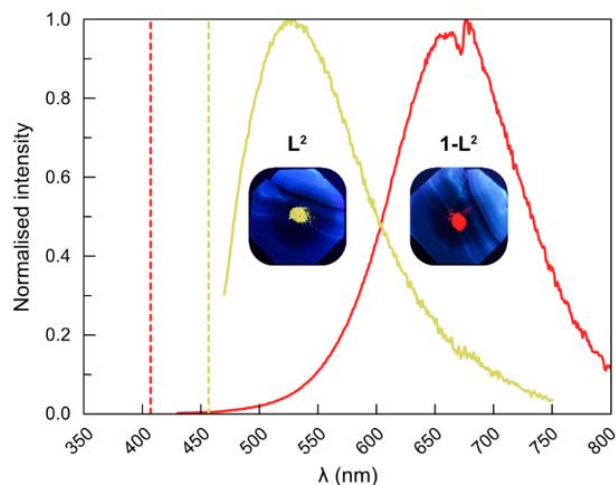


Fig. 2. A) Emission spectra, with normalised intensity, of L^2 (yellow line) and 1L^2 (red line); dashed lines represent the maximum of excitation (λ_{exc} in Table 1). Photographs of the ligand and complex taken upon UV irradiation are also shown. B) Molecular structure of complex 1L^2 (Hs omitted for clarity) highlighting the different fragments: EWO (fluorinated chalcone) in ellipsoids, PdCl_2 in ball and stick while PCy_2 is in capped stick representation. Colour atom code: Pd (deep blue), Cl (green), P (orange), O (red), F (light blue), C (grey). Relevant distances in Å: Pd-Cl = 2.3083(8); Pd-P = 2.3295(7); C-C (olefin) = 1.324(4).

The data for the metal complexes in Table 1 show that P-coordination to the MX_2 fragment drastically affects the luminescence of the compounds. The coordination introduces σ -donation from the P atom to M and π -backdonation from M to P as additional modifiers of electron density on the P atom and, eventually, on the chalcone. The result on the PdX_2 complexes 1L^{1-4} and 3L^1 is that they show orange-reddish

emissions in the short 643–680 nm range for maxima. This suggests that the inductive R effect is in good part derived towards modified P donation of the coordination bond. Overall, coordination diminishes the electron density available at P for the interactions with the chalcone fragment. The observed result is higher λ_{emis} values for complexes than for free ligands.

Table 1. Excitation and emission data of the ligands and complexes in the solid state. Instability of L^3 (when non-coordinated) precludes the corresponding luminescence analyses.

Entry/ Comp.	λ_{exc} (nm)	λ_{emis} (nm) ^a	Φ (%)	τ_{av} (ns) ^b
1/ L^1	413	606	10.1	2.4
2/ L^2	460	530	4.1	3.5
3/ L^4	472	552	< 3	3.0
4/ 1L^1	405	649	28.0	1.3×10^3
5/ 1L^2	412	676	21.8	1.6×10^3
6/ 1L^3	405	643	15.6	1.4×10^3
7/ 1L^4	469	680	< 3	6.4×10^2
8/ 2L^1	Undetected emission			
9/ 3L^1	415	666	15.7	5.4×10^3
10/ 4L^1	Undetected emission			
11/ 5L^1	Undetected emission			

^a Very broad emission bands. ^b $\tau_{\text{av}} = (A_1\tau_1^2 + A_2\tau_2^2 + \dots) / (A_1\tau_1 + A_2\tau_2 + \dots)$

A positive effect of complexation to PdCl_2 (or PdBr_2 in the case of 3L^1) is the extraordinary increase of the Φ range to 15–28 % values. Again, the 1L^4 complex is hardly luminescent, supporting the importance of fluorine substituents in the chalcone ring for the emissive properties.²⁷ Moreover, Figure 2 shows the particular example of the Cy-PEWO- F_4 ligand L^2 and its corresponding PdCl_2 complex 1L^2 . The photographs taken upon UV irradiation allow to distinguish the different emission of both compounds: yellow for the ligand and deep orange for the complex. Note that the emission bands are very broad and the λ_{emis} is not enough to guess the colour (L^1 is yellowish upon irradiation too, see Figure ES13). Remarkably, this colour change is linked to a substantially higher Stokes shift for 1L^2 than for L^2 (*i.e.* $9.5 \times 10^3 \text{ cm}^{-1}$ and $2.9 \times 10^3 \text{ cm}^{-1}$) and longer lifetimes (in the order of ms for the complexes and ns for the ligands). These observations suggest a plausible luminescence switch from fluorescence to phosphorescence upon coordination to PdCl_2 .²⁸

We were also intrigued about the orbital differences that produce the lethal effect on the luminescent behaviour of the $\text{Pd}(\text{CN})_2$ (4L^1) and PtCl_2 (5L^1) variants of the strongly emitting and structurally analogous PdCl_2 (1L^1) complex. Whereas 1L^1 (and the PdBr_2 compound 3L^1) have two medium-strength σ -donor and slightly π -donor halide ligands, 4L^1 has more σ -donor and very strongly π -acceptor cyanide ligands. On the other hand, 5L^1 has Pt instead of Pd, and the lanthanide contraction along with the relativistic effects in Pt produce large orbital energy differences between the two isoelectronic metal centres.²⁹ The two cases of 4L^1 and 5L^1 are in the end roughly similar in that they are expected to have a metal centre more greedy of electron density and, consequently, less prone to be polarized.

In order to confirm our qualitative hypotheses and identify the orbitals involved in the emission, DFT calculations were carried out. Particularly, we focussed the attention in the ligand Ph-PEWO- F_4 (L^1) and the derived complexes 1L^1 (luminescent) and $\text{4L}^1/\text{5L}^1$ (non-luminescent). As that the emissions observed do not appear in solution, geometry optimizations in the gas phase were carried out using the X-ray structures as initial guesses, leading to minimal modifications of the solid structures (full description of the computational details can be found in the ESI). First, the simulation of the absorption spectra using time-dependent DFT (TD-DFT) allows to assign the electronic transitions responsible for the excitation maxima observed in L^1 and 1L^1 . Specifically, the computed HOMO-LUMO gap fits well the λ_{exc} experimentally measured for L^1 ($\lambda_{\text{calc}} = 402 \text{ nm}$; $\lambda_{\text{exp}} = 413 \text{ nm}$). While the HOMO orbital is mainly located in the Ph_2P moiety (87%), the LUMO is purely a chalcone orbital (see Figure ES15). Also, the experimental λ_{exc} maximum of 1L^1 (*i.e.* 405 nm) fits satisfactorily the calculated transition from the HOMO-2 to the LUMO orbital ($\lambda_{\text{calc}} = 395 \text{ nm}$). In both cases the contribution of the different fragments highlighted in Figure 3 is as follows: (58% Ph_2P , 22% PdCl_2 , 20% EWO) for HOMO-2, and (42% PdCl_2 , 38% EWO, 20% Ph_2P) for LUMO; both are symmetrical instead of predominantly located in one of the two ligands. Remarkably, a similar transition (HOMO-2 to LUMO) in the Pt analogue 5L^1 is computed to be markedly more energetic (*i.e.* 349 nm) while the HOMO-LUMO transition for PdCN_2 complex 4L^1 should originate a band at a similar wavelength (*i.e.* 350 nm), confirming the qualitative interpretation of similar behaviour of these two complexes.

Using TD-DFT, the emission experimentally observed for 1L^1 ($\lambda_{\text{exp}} = 649 \text{ nm}$) was assigned to the monodeexcitation from the first triplet state (T_1), computed to be very similar ($\lambda_{\text{calc}} = 667 \text{ nm}$). The emission band mainly involves the LUMO→HOMO phosphorescent transition (Figure 3). This is perfectly consistent with the high Stokes shift and long lifetime values commented previously (Table 1). It is worth remarking that geometry relaxation was discarded due to the very limited structural deformability allowed in the solid state.³² Moreover, the fluorescent emissions as well as other potentially phosphorescent ones, were also computed and subsequently discarded because of numerical results far from the experimental data (details in ESI).

Evidently, deexcitation from the LUMO (42% PdCl_2 , 38% EWO, 20% Ph_2P) to the PdCl_2 HOMO, responsible for the orange-emitting behaviour of 1L^1 , is drastically affected either in the $\text{Pd}(\text{CN})_2$ or PtCl_2 analogues. Figure 3 gathers the frontier molecular orbitals (FMOs) for 1L^1 , 4L^1 and 5L^1 for comparison. Interestingly, the computed phosphorescent emissions (decay from triplet states) are experimentally unobservable, as direct consequence of the changes in the FMOs. For 5L^1 , the PtCl_2 HOMO resembles its PdCl_2 analogue but the contribution of the PtCl_2 fragment in the LUMO drops to the 7% (*vs* 42% for 1L^1) and the deexcitation from the first triplet is computed to be much more energetic (*i.e.* 555 nm). The effect of the Cl by CN substitution in FMOs is also clear, with reduced participation of the $\text{Pd}(\text{CN})_2$ fragment in the LUMO of 4L^1

(casually similar to the PtCl_2 compound) and negligible in the HOMO (Figure 3 below). After the identification of the key orbitals involved in the luminescent behaviour (mainly located in the PdCl_2 fragment) the data of Table 1 can be better rationalized: *i*) both the PdBr_2 substitution in $\mathbf{3L}^1$ (Br is well known to be electronically very similar to Cl) or the R_2P modification in $\mathbf{1L}^2$ and $\mathbf{1L}^3$ move in the range of variations of polarization; *ii*) totally different emissions (in fact experimentally undetectable) must be expected from the $\text{Pd}(\text{CN})_2$ ($\mathbf{4L}^1$) or PtCl_2 ($\mathbf{5L}^1$) congeners, with LUMOs hardly participated by their MX_2 moieties.

Finally, the computed deexcitations from the triplet states are not able to explain the experimentally observed emission of the Ph-PEWO- F_4 free ligand (\mathbf{L}^1 , $\lambda_{\text{exp}} = 606 \text{ nm}$) discarding the phosphorescent behaviour in that case. However, $\text{S}_1 \rightarrow \text{S}_0$ transition from a singlet state where a slight bending of the chalcone group is observed, afforded a satisfactory value of fluorescent emission at $\lambda_{\text{calc}} = 580 \text{ nm}$, strongly supported by the short lifetime of *ca.* 2 ns. In this case, the contribution of the R_2P fragment in the orbitals involved is significant (details in ESI), and consequently the effect of the Cy substitution is appreciable (data in Table 1).

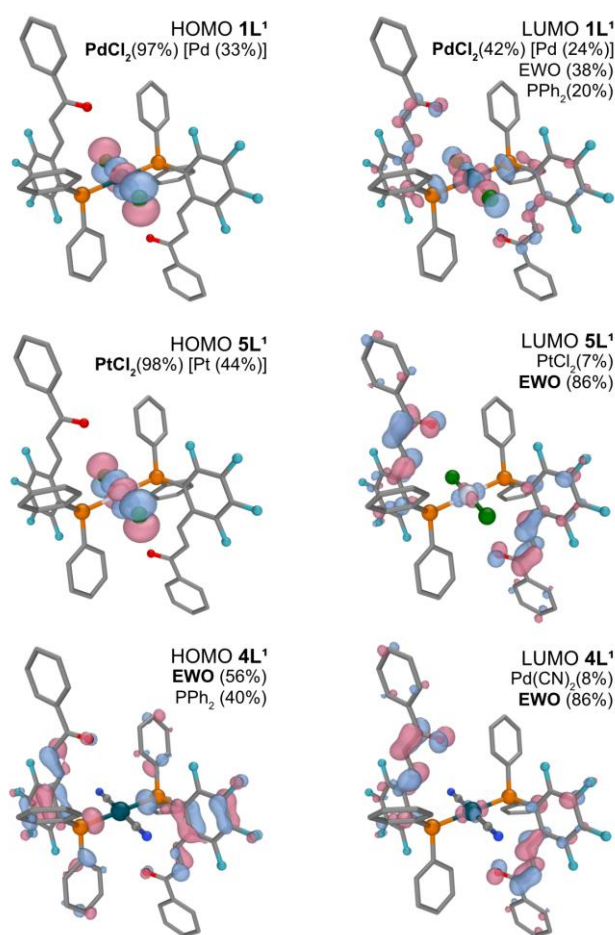


Fig. 3. FMOs of complexes $\mathbf{1L}^1$ (above), $\mathbf{5L}^1$ (middle) and $\mathbf{4L}^1$ (below). Contribution percentages of the different fragments are included, with the main participation in each case highlighted in bold. Relevant contributions of the metal atom (when higher than 10%) are also showed.

In summary, we have reported here a family of intensely phosphorescent palladium(II) complexes of the type *trans*-

$[\text{PdX}_2\text{L}_2]$ ($\text{L} = \text{R-PEWO-F}_4$; $\text{X} = \text{Cl, Br}$) with quantum yields (Φ) above 15%. The orange emission is only observed in the solid state and is remarkably similar modifying the substituents in the ligand (R_2P moiety with $\text{R} = \text{Ph, Cy, iPr}$) but the lack of fluorination in the chalcone-EWO group is clearly detrimental for the luminescent behaviour. Conversely, the non-emitting $\text{Pd}(\text{CN})_2$ and PtCl_2 analogues lack the metal/chalcone connection in the LUMO orbital, directly involved in the luminescence observed for the structurally identical PdCl_2 (or PdBr_2) derivatives. DFT studies have satisfactorily reproduced the excitation and emission properties of the model compound $\mathbf{1L}^1$ and have allowed to rationalize the experimental observations upon analysis of the group contribution (R_2P , EWO & MX_2) in the key orbitals. Yellow fluorescent emission, supported by lower Stokes shifts and shorter lifetimes is also detected for the free R-PEWO- F_4 ligands, again intimately related with the chalcone skeleton of the EWO moiety.

We thank the Spanish MCINN (Projects PID2020-118547GB-I00 and PGC 2018-093863-B-C21) for the funding provided. J. P.-de-L. also acknowledges MCINN for a FPI studentship (BES-2017-080726). M. N. P.-D. thanks Dr. Eric Mates-Torres for help and the UVA for a Margarita Salas postdoctoral fellowship (ref. CONVREC-2021-221).

Conflicts of interest

There are no conflicts to declare.

Notes and references

- For reviews see: a) C. Zhuang, W. Zhang, C. Sheng, W. Zhang, C. Xing and Z. Miao, *Chem. Rev.*, 2017, **117**, 7762–7810. b) N. A. A. Elkanzi, H. Hrichi, R. A. Alolayan, W. Derafa, F. M. Zahou and R. B. Bakr, *ACS Omega*, 2022, **7**, 27769–27786; c) S. L. Gaonkar and U. N. Vignesh, *Res. Chem. Intermed.*, 2017, **43**, 6043–6077.
- For reviews see: a) K. G. Komarova, S. N. Sakipov, V. G. Plotnikov and M. V. Alifimov, *J. Lumin.*, 2015, **164**, 57–63. b) P. Mahesha, N. S. Shetty and S. D. Kulkarni, *J. Fluoresc.*, 2022, **32**, 835–862.
- S. Kagitkar and D. Sunil, *Chem. Pap.*, 2021, **75**, 6147–6156.
- X. Cheng, F. Yang, J. Zhao, J. Ni, X. He, C. Zhou, J. Z. Sun and B. Z. Tang, *Mater. Chem. Front.*, 2020, **4**, 651–660.
- L. J. Gomes, T. Moreira, L. Rodriguez and A. J. Moro, *Dyes Pigm.*, 2022, **197**, 109845.
- A.-T. Mohammad and W. R. Abbas, *RSC Adv.*, 2021, **11**, 38444–38456.
- E. Gioria, J. M. Martinez-Illarduya, D. Garcia-Cuadrado, J. A. Miguel, M. Genov and P. Espinet, *Organometallics*, 2013, **32**, 4255–4261.
- M. N. Peñas-Defrutos, A. Vélez, E. Gioria and P. Espinet, *Organometallics*, 2019, **38**, 4701–4707.
- X. Luo, H. Zhang, H. Duan, Q. Liu, L. Zhu, T. Zhang and A. Lei, *Org. Lett.*, 2007, **9**, 4571–4574.
- E. Gioria, J. del Pozo, J. M. Martínez-Illarduya and P. Espinet, *Angew. Chem., Int. Ed.*, 2016, **55**, 13276–13280.
- E. Gioria, J. del Pozo, A. Lledós and P. Espinet, *Organometallics*, 2021, **40**, 2272–2282.
- J. Ponce-de-León and P. Espinet, *Chem. Commun.*, 2021, **57**, 10875–10878.
- M. N. Peñas-Defrutos, A. Vélez and P. Espinet, *Organometallics*, 2020, **39**, 841–847.

²² A. Roque, J. C. Lima, A. J. Parola and F. Pina, *Photochem. Photobiol. Sci.*, 2007, **6**, 381–385.

²⁴ H. Zhang, X. Luo, K. Wongkhan, H. Duan, Q. Li, L. Zhu, J. Wang, A. S. Batsanov, J. A. K. Howard, T. B. Marder and A. Lei, *Chem. - Eur. J.* 2009, **15**, 3823–3829.

²⁵ For an example of luminescent chalcones in the solid state but not in solution see: L. Zhang, J. Liu, J. Gao, R. Lu and F. Liu, *RSC Adv.*, 2017, **7**, 46354–46357.

²⁶ Excitation spectra are not informative, due to line scattering.

²⁷ J. Ponce-de-León, R. Infante and P. Espinet, *Chem. Commun.*, 2021, **57**, 5458–5461.

²⁸ J. M. Forward, D. Bohmann, J. P. Fackler Jr and R. J. Staples, *Inorg. Chem.*, 1995, **34**, 6330–6336.

²⁹ This is reflected, for instance, in the 1st ionization energy of Pt (870 kJ/mol), considerably higher than Pd (804 kJ/mol), which exemplifies the general reluctance of Pt to diminish its electron density in shared bonds, compared to Pd.

³² Reoptimization of both S₁ and T₁ states led to profound structural change, presumably not accessible in the crystal.